ARTICLE IN PRESS

Available online at www.sciencedirect.com
SCIENCE DIRECT®

Advances in Space Research xxx (2005) xxx–xxx

ADVANCES IN SPACE RESEARCH (a COSPAR publication)

www.elsevier.com/locate/asr

Long-term predictability of orbits around the geosynchronous altitude

S. Breiter [a], I. Wytrzyszczak [a,*], B. Melendo [b]

[a] *Astronomical Observatory of A. Mickiewicz University, ul. Sloneczna 36, PL 60-286 Poznań, Poland*
[b] *Grupo de Mecánica Espacial, Universidad de Zaragoza, E 50009 Zaragoza, Spain*

Received 28 October 2004; received in revised form 15 February 2005; accepted 15 February 2005

Abstract

For a family of simulated geostationary, geosynchronous and super-geostationary orbits we compute the indicator called MEGNO in order to find out which orbits are chaotic and the timescale of their exponential divergence. A symplectic integrator of the Wisdom–Holman type was used for this purpose, with an integration span of 40 years. The results indicate that chaotic orbits exist only at the separatrix between geostationary libration and circulation and that they are relatively rare. The super-geostationary region seems to be entirely regular and quasi-periodic on the timescale of few decades.

Keywords: Satellite orbits; Artificial Earth satellites; Space debris

1. Introduction

The question of the geosynchronous Earth orbits (GEO) dynamics is of particular interest from both theoretical and practical points of view. Of course, the same concerns the super-GEO objects that are mostly the disposed satellites from the geostationary ring. According to Flury et al. (2000), the geostationary ring is a segment of a spherical shell spanning around the equatorial orbit with the reference radius $A = 42{,}164$ km. The segment is about 150-km thick in the radial direction, and $\pm 15°$ wide in latitude. The recommended super-GEO orbits should have perigees higher than $A + 235$ km plus a correction depending on their area-to-mass ratio.

Great effort has been made to solve the problem of possible re-entry of the super-GEO objects into the geostationary belt, that might increase the collision risk (Yasaka et al., 1999; Pardini and Anselmo, 2001; Wytrzyszczak, 2004). In the present paper, we raise a slightly different, although equally important question: are the GEO and super-GEO objects predictable? How fast does some uncertainty of their position and velocity grow in time? For this purpose we use the modern chaoticity indicator called MEGNO (mean exponential growth factor of nearby orbits), introduced by Cincotta et al. (2003). Symplectic numerical integration of the satellites motion combined with the evolution of related tangent maps allowed us to generate the MEGNO maps that show the regularity or chaoticity of motion for a wide range of initial conditions.

2. The model and numerical integration method

We studied the motion of a presumably spherical satellite under the action of the Earth's gravity field, lunisolar perturbations and direct radiation pressure. The geopotential included spherical harmonics up to degree and order 4 of the EGM96 model (Lemoine et al., 1987) Positions of the Sun and the Moon required for

* Corresponding author. Tel.: +48 61 8292774; fax: +48 61 8292772.
E-mail address: iwona@amu.edu.pl (I. Wytrzyszczak).

0273-1177/$30
doi:10.1016/j.asr.2005.02.033

the evaluation of the perturbing forces were computed according to the simplified formulas from The Astronomical Almanac (2000, pp. C1 and D46). For the purpose of the solar radiation force evaluation, we have assumed the satellites to be spherical objects with an area-to-mass ratio 0.005 $m^2\,kg^{-1}$ and a reflectivity coefficient 1.14. The influence of the shadow function was neglected in our simulation.

Canonical equations of motion were considered in the geocentric reference frame rotating with the Earth. The Hamiltonian function $\mathscr{H}$ of the problem was partitioned into the leading part $\mathscr{H}_0$, describing the Keplerian problem in the rotating reference frame, and the perturbing part $\mathscr{H}_1$, consisting of the contributions due to the perturbing part of the geopotential $V_\oplus$, lunisolar terms $V_\odot + V_m$, and the radiation pressure potential $V_{\rm rp}$. So we have

$$\mathscr{H} = \mathscr{H}_0 + \mathscr{H}_1, \tag{1}$$

$$\mathscr{H}_0 = \frac{\vec{R}^2}{2} - \Omega_\oplus(xY - yX) - \frac{\mu}{r}, \tag{2}$$

$$\mathscr{H}_1 = V_\oplus(\vec{r}) + V_\odot(\vec{r},t) + V_m(\vec{r},t) + V_{\rm rp}(\vec{r},t), \tag{3}$$

where $\Omega_\oplus$ is the Earth rotation rate, and μ is the geocentric gravity parameter. The evolution of coordinates $\vec{r} = (x,y,z)$ and of their conjugate momenta $\vec{R} = (X,Y,Z)^{\rm T}$ is described by the canonical equations of motion

$$\frac{{\rm d}\vec{r}}{{\rm d}t} = \frac{\partial\mathscr{H}}{\partial\vec{R}}, \quad \frac{{\rm d}\vec{R}}{{\rm d}t} = -\frac{\partial\mathscr{H}}{\partial\vec{r}}. \tag{4}$$

In order to integrate the equations of motion (4), the 4th order symplectic integrator of Yoshida (1993) was applied with the Wisdom–Holman type partition of the Hamiltonian described above (Wisdom and Holman, 1991). This kind of integrator is necessarily a fixed-step procedure and we have assumed it to be about 1/20 of the orbital period. This value was sufficient for small eccentricity orbits. Some orbits open to the possibility of a significant eccentricity growth were also verified using a smaller stepsize.

3. The MEGNO definition and computation

The fundamental property of a chaotic orbit is the exponential growth of the infinitesimal position/momentum error $\vec{\delta}$. With an initial value $\vec{\delta}_0$ of such a vector we have, asymptotically, $\delta \propto \delta_0 \exp \sigma t$, where σ is the largest Lyapunov characteristic exponent (LCE). Thus, an associated quantity $T_{\rm L} = \sigma^{-1}$, the Lyapunov time, tells us how much time a small error requires to increase by a factor $\exp(1) \approx 2.72$. By rule of thumb, motion is considered unpredictable on a timescale longer than 10 $T_{\rm L}$.

Briefly, the MEGNO indicator Y is a time-weighted LCE (Cincotta et al., 2003)

$$Y(t) = \frac{1}{t}\int_0^t \frac{2}{t'}\left(\int_0^{t'} \frac{\dot{\delta}}{\delta} t''{\rm d}t''\right){\rm d}t'. \tag{5}$$

The behavior of MEGNO depends on the type of motion:

(1) for a chaotic orbit it asymptotically tends to $Y \approx \frac{\sigma}{2}t$;
(2) for a non-chaotic, quasi-periodic orbit $Y \to 2$;
(3) for stable, isochronous periodic orbits $Y \to 0$.

A definite advantage of MEGNO is its fast convergence, at least 10 times better than for a numerically estimated LCE. However, computing MEGNO over a relatively short time interval reveals the differences between the convergence rate of Y in various domains of the phase space. According to our experience, trajectories close to stable periodic orbits will have $Y < 2$ (often negative), and trajectories in the neighborhood of unstable periodic orbits will have $2 < Y \lesssim 3$.

In order to evaluate the MEGNO value of a given satellite orbit, we have treated the symplectic integrator as a discrete variable mapping. For each integrator step, an associated tangent map was followed, in order to obtain the evolution of the initial error vector $\vec{\delta}_0$. The 'MEGNO for maps' algorithm was applied as given by Cincotta et al. (2003). For the Keplerian part of the Wisdom–Holman scheme, we used the tangent map of Mikkola and Innanen (1999). The tangent maps of the perturbations 'momentum kicks' were evaluated according to the Hessian matrices of the respective potentials.

An important remark concerns the choice of $\vec{\delta}_0$: contrary to Goździewski et al. (2001), who emphasized the random choice of this vector, we maintained the same initial value of $\vec{\delta}_0$ for all sampled initial conditions of $\vec{r},\vec{R}$. This results in some artificially created zones of low MEGNO values due to the proximity of $\vec{\delta}_0$ to the minimum Lyapunov exponent direction. However, such patterns can be easily identified and they practically do not influence the detection of chaotic orbits.

For the purpose of our study, we decided to simulate orbits over 40 years of motion, i.e. more than 10^4 of fundamental $24^{\rm h}$ periods. This is a relatively short time, but the necessity of evaluating tangent maps together with the trajectory, increases the computational cost. The simulation of a 40 years interval with a time step 0.05 d takes from 10 s (geopotential only) to 15 s (all perturbations) on a 2 GHz PC. But, according to our experiments, this expense pays off because replacing tangent maps with a "shadow trajectory" (known also as "two particles") approach degrades the accuracy and requires longer integration intervals to be followed. Fig. 1 shows the behavior of $Y(t)$ over 400 years for three

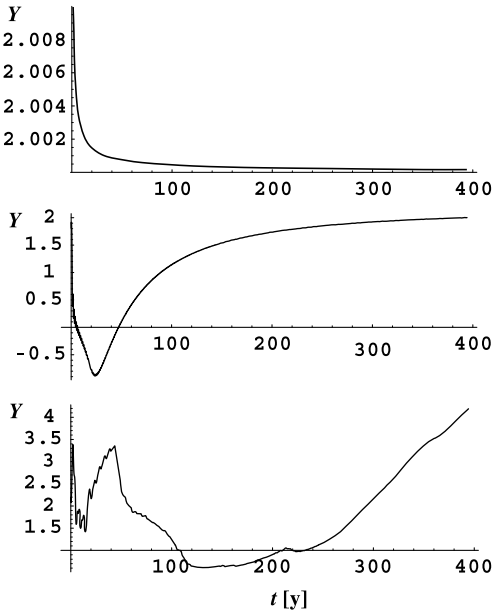

Fig. 1. MEGNO as a function of time for three exemplary orbits.

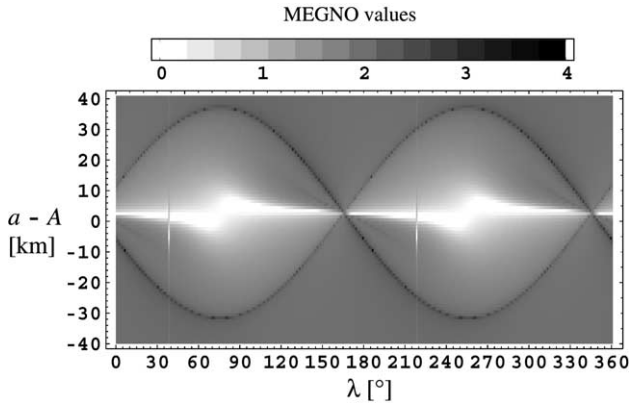

Fig. 2. MEGNO as a function of initial longitude and semi-major axis. All perturbing effects excluded, except for the second degree harmonics.

exemplary orbits. The first one (top) is clearly quasi-periodic and it had $Y(t_1) = 2.001$ after $t_1 = 40$ year; we can see, that the MEGNO converges to $Y = 2$. The second example (middle) shows an orbit with a low $Y(t_1) = -0.57$; it converges to $Y = 2$ but more slowly than the previous one, and with $Y < 2$ all the time. The last example (bottom) had $Y(t_1) = 3.38$; the orbits of this kind are problematic and there is no rule their future MEGNO obeys. Sometimes their Y grows systematically, but sometimes it oscillates close to 3 or 4 even over 4000 years. Even when they prove chaotic, their Lyapunov times are long, so we classify them as 'mildly chaotic'.

4. Results

4.1. Longitude – semi-major axis map

Our first study considered a family of orbits with all initial elements fixed, but with various values of the initial semi-major axis a and of the initial right ascension of the ascending node Ω. The remaining elements at the initial epoch $t_0 = \mathrm{JD2000} + 97^{\mathrm{d}}$, were $e = 0.0003$ for the eccentricity, $i = 0$ for the inclination, $M = 0$ for the mean anomaly, and $\omega = 0$ for the argument of perigee. With these initial elements, we had the initial mean longitude equal to the initial right ascension of the ascending node $\Omega = \lambda$, hence we are going to speak about the map of MEGNO values on the (λ, a) parametric plane. This map is of primary importance, because the 1:1 tesseral resonance, that is the central feature of the GEO dynamics, has λ as a critical angle and $L = \sqrt{\mu a}$ as its conjugate momentum.

Fig. 2 presents the values of MEGNO obtained after symplectic integration on the interval of about 40 years. More precisely, we followed 14,400 orbital periods computed from the initial semi-major axes according to Kepler's third law. All perturbing effects were turned off, save for the second degree harmonics of the geopotential, with the $C_{2,0}$, $C_{2,2}$, and $S_{2,2}$ coefficients. The mean longitude grid was 1° and the semi-major axis grid was 1 km, spanning the $A \pm 40$ km range. Inspecting Fig. 2, we notice the well known pendulum-like pattern related to the libration zones of the GEO resonance. Two stable stationary points are visible at longitudes of about 75° and 255°, as well two unstable points at 165° and 345°. There are two kinds of low MEGNO artifacts related to the use of a common $\vec{\delta}_0$ for all initial conditions: thin vertical stripes at $\lambda = 38°$ and $\lambda = 218°$, tadpole shaped pairs with 'heads' close to the stable stationary points and 'tails' originating at the unstable points. Apart from these features, most of the parametric plane is dominated by quasi-periodic orbits with $Y \approx 2$. Only the separatrix contains irregularly distributed orbits with $2 < Y < 4$ that mark the presence of unstable periodic orbits. The overall picture can be qualified as practically regular.

Adding more harmonics of the geopotential we affect the symmetry of the libration zones, but MEGNO at the separatrices does not exceed 4.2, even after including the radiation pressure effects. It is the addition of lunisolar perturbations that leads to the appearance of clearly chaotic orbits. Fig. 3 presents the values of MEGNO after 40 years with the mean longitude grid of 2° and the semi-major axis grid of 1 km. The initial semi-major axes extend from below the GEO radius, 42,116 km up to the super-GEO disposal orbits zone, at 42,416 km. The values of MEGNO among the 54,000 sample orbits were $-1.39 < Y < 8.04$, but the shades in Fig. 3 are clipped to the $0 \leqslant Y \leqslant 6$ range in order to enhance details.

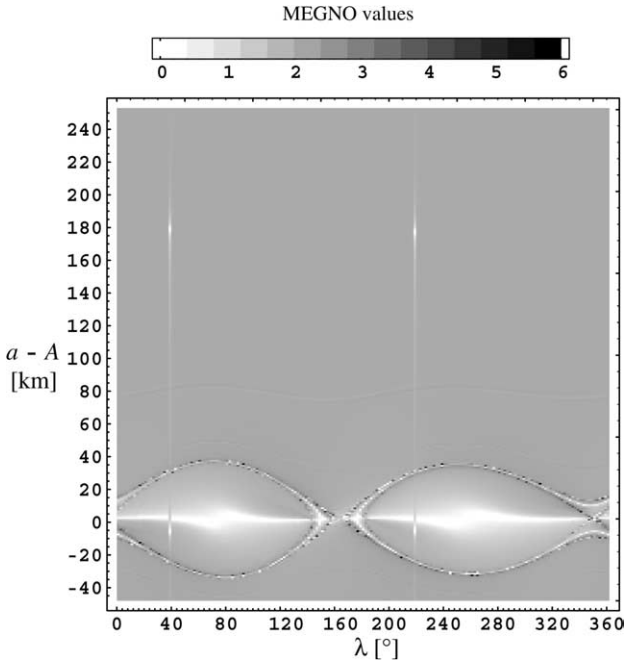

Fig. 3. MEGNO as a function of initial longitude and semi-major axis.

Due to the lunisolar perturbations, the separatrix between the inner circulation, libration, and outer circulation regions is thick and contains irregularly spaced chaotic orbits. A blow-up of the region close to the unstable geostationary point is shown in Fig. 4.

Once the chaotic orbits in our problem have been spotted, the question should be raised what do they look like? The answer can be found in Figs. 5 and 6. We have chosen an orbit ("orbit 1") with $a = 42{,}158.255$ km and

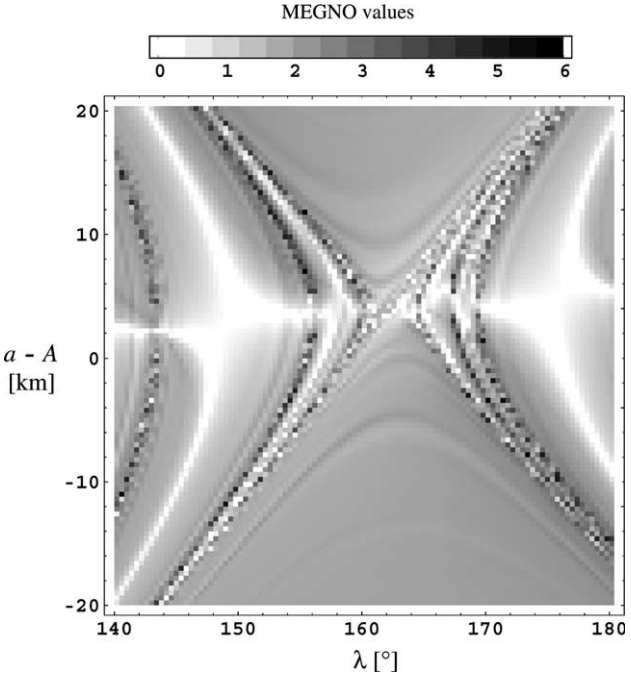

Fig. 4. The blow-up of Fig. 3 close to the unstable geostationary point.

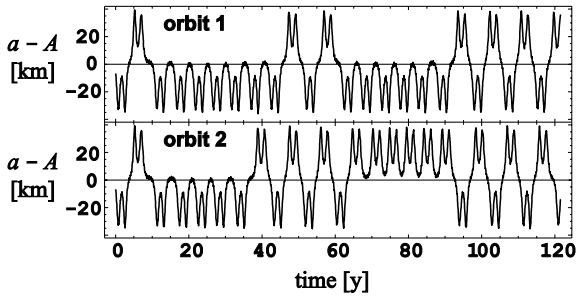

Fig. 5. Osculating semi-major axes of two exemplary nearby orbits.

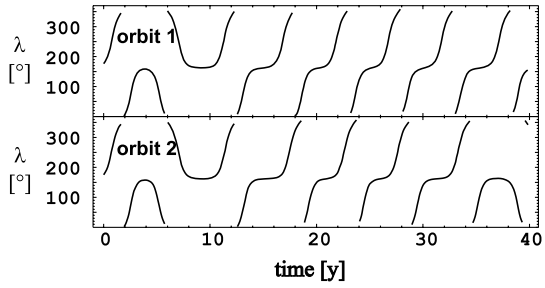

Fig. 6. Mean longitude for the orbits presented in Fig. 5.

$\lambda = \Omega = 176°$, with the MEGNO value close to 5. Such an orbit should be mildly chaotic. We also simulated a nearby orbit ("orbit 2") with a slightly different initial semi-major axis $a = 42{,}158.254$ km (and the same values of remaining elements), in order to see the sensitivity of motion with respect to the initial conditions.

Fig. 5 presents the evolution of the osculating semi-major axes of both orbits on the extended interval of 120 years. The most important chaos-related feature is the phenomenon of intermittency: both orbits swap between different regimes of motion. Let us use the labels L, I, O for the libration, inner circulation (below the GEO radius), and outer circulation (above the GEO radius), respectively. Then, orbit 1 takes the itinerary

(ILIIIII)ILLIIIIILLLL,

whereas orbit 2 follows

(ILIIIIL)LLOOOOOLLL.

The brackets mark the first 40 years of motion; for this interval we plot the mean longitude λ of both orbits in Fig. 6. As we see, due to different itineraries of the two nearby orbits, the difference between the two longitudes reached almost 180°. In a purely Keplerian motion or for a non-chaotic perturbed orbit, such separation in λ due to the semi-major axes difference of 1 m would be attained in 4×10^4 years. The Lyapunov time estimated from the MEGNO is indeed few years and our results agree with the rule of thumb given in Section 3.

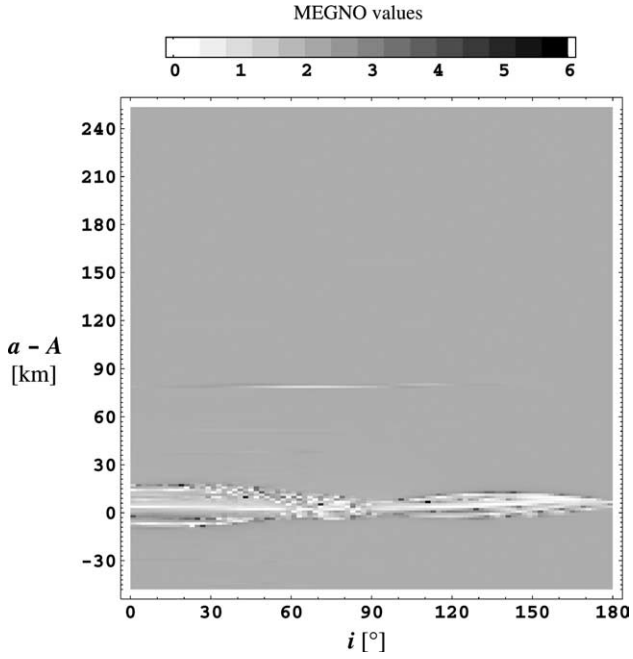

Fig. 7. MEGNO as a function of initial inclination and semi-major axis.

4.2. Inclination, eccentricity and semi-major axis

Fig. 7 presents the MEGNO map that we obtained scanning a grid of initial inclinations ($0 \leqslant I \leqslant 180°$) and major semi-major axes ($42{,}116 \leqslant a \leqslant 42{,}416$ km). The grid resolution was 2° in I and 1.5 km in a. For all orbits we set $e = 0.0003$ and $M = \omega = \Omega = 0$. The highest value of MEGNO in this sample was $Y = 6.1$ on the interval of 14,400 orbital periods. As seen in Fig. 7, chaotic orbits are quite few, and all are located at almost geosynchronous values of a. On the other hand, there is no preference with respect to the inclinations.

Similarly to the (I, a) plot, we also investigated the (e, a) map with small eccentricities ($e \leqslant 0.1$) of an equatorial orbit. No unexpected phenomena were detected: the zone of a close to A created a stripe of low MEGNO values with occasional chaotic orbits. No significant dependence on e was seen. The maximum MEGNO we observed was 8.6, but still chaotic orbits were rather exceptional.

5. Conclusions

Our computations of MEGNO indicate that there exist chaotic orbits in the geostationary region, with the Lyapunov times short enough to make a 40 years prediction impossible. Such orbits however are rare and appear only close to the separatrix between the geostationary libration and circulation modes. The chaos is rather mild, manifested through the phenomenon of intermittency between different libration and circulation regimes. The underlying mechanism is the interaction of lunisolar perturbations with the 1:1 tesseral resonance, resulting in a small thickness of the separatrix; there are no signs of overlapping resonances that might introduce a wide chaotic zone (Lichtenberg and Lieberman, 1983). All the super-GEO orbits that we simulated are regular quasi-periodic, as far as small inclinations or eccentricities are concerned.

Acknowledgement

The research was sponsored by the Polish State Committee of Scientific Research (KBN) Grant 5T12D 02623.

References

Cincotta, P.M., Giordano, C.M., Simó, C. Phase space structure of multi-dimensional systems by means of the mean exponential growth factor of nearby orbits. Physica D 182, 151–178, 2003.

Flury, W., Massart, A., Schildknecht, T., Hugentobler, U., Kuusela, J., Sodnik, Z. Searching for small debris in the geostationary ring. ESA Bulletin 104, 92–100, 2000.

Goździewski, K., Bois, E., Maciejewski, A.J., Kiseleva-Eggleton, L. Global dynamics of planetary systems with the MEGNO criterion. Astronomy and Astrophysics 378, 569–586, 2001.

Lemoine, F.G., Kenyon, S.C., Factor, J.K., Trimmer, R., Pavlis, N.K., Chinn, D.S., Cox, C.M., Klosko, S.M., Luthcke, S.B., Torrence, M.H., Wang, Y.M., Williamson, R.G., Pavlis, E.C., Rapp, R.H., Olson, T.R. The development of the joint NASA GSFC and NIMA geopotential model EGM96. Tech. Rep. NASA/TP-1998-206861, NASA Goddard Space Flight Center, Greenbelt, Maryland, 20771 USA, 1987.

Lichtenberg, A.J., Lieberman, M.A. Regular and Stochastic Motion. Springer, Berlin, 1983.

Mikkola, S., Innanen, K. Symplectic tangent map for planetary motions. Celestial Mechanics and Dynamical Astronomy 74, 59–67, 1999.

Pardini, C., Anselmo, L. Influence of the spacecraft end-of-life reorbiting altitude on the long-term collision risk in the geostationary ring. Advances in Space Research 28, 1403–1408, 2001.

The Astronomical Almanac. Nautical Almanac Office, Washington and London, 2000.

Wisdom, J., Holman, M. Symplectic maps for the n-body problem. Astronomical Journal 102, 1528–1538, 1991.

Wytrzyszczak, I. Testing the safety of decommissioned spacecraft above GEO. Advances in Space Research 34, 1209–1213, 2004.

Yasaka, T., Hanada, T., Hirayama, H. GEO debris environment: a model to forecast the next 100 years. Advances in Space Research 23, 191–199, 1999.

Yoshida, H. Recent progress in the theory and application of symplectic integrators. Celestial Mechanics and Dynamical Astronomy 56, 27–44, 1993.